SPACECRAFT FIBERGLASS STRUT CHARGING/DISCHARGING AND EMI*

K.G. Balmain and M. Gossland**
Department of Electrical Engineering
University of Toronto
Toronto, Canada M5S 1A4

K. Karia
Spar Aerospace Limited
1700 Ormont Drive
Toronto, Canada M9L 2W7

Abstract

Glass-fiber-epoxy struts used in spacecraft extendable masts were exposed to a 20 keV electron beam. Discharges were observed, and near-field measurements used to deduce the radiated emission spectrum for comparison with spacecraft specifications.

Introduction

Glass-fiber-epoxy struts are used as the basic structural elements in spacecraft extendable masts intended primarily for the support of solar cell arrays. In synchronous orbit, these struts could accumulate charge from the energetic-electron environment and then arc-discharge, creating electromagnetic interference which could affect spacecraft control and communication systems. This situation differs from many others which have been studied, in that the dielectric material is not in contact with the metallic structure of the spacecraft. The objective of this paper is to estimate whether or not the spacecraft radiated emission specifications will be exceeded by broadband emissions from arcs on the struts.

Experimental Procedures and EMI Estimation

The interference threat was evaluated by the laboratory study of extreme cases, namely the exposure of strut specimens to a 20 keV electron beam at current densities of 3 and 10 nA/cm². These current densities are one to two orders of magnitude higher than the values expected in synchronous orbit, and the beam is monoenergetic rather than being more realistically broad-spectrum. The effect of this is to produce results which are decidedly "worst case". The strut specimens were 10 cm long with square cross-sections 3.5 mm x 3.5 mm. Each specimen included a typical aluminum stud secured with conducting epoxy. The specimens were mounted on a bracket 1 cm over a conducting substrate as shown in Fig.1 which also shows a loop antenna between the strut and the substrate.

One end of the loop was connected via a 47-ohm cable-matching resistor to a 50-ohm cable which in turn was connected to the 50-ohm input of an oscilloscope. The other end of the loop was grounded to provide the lowest impedance path possible to ground. The intent of this was to allow induced charge on the loop or blowoff charge incident on the loop to drain preferentially to ground rather than passing into the measurement line, so that the measured signal would be proportional to the time derivative of the loop flux, hence the arc current along the strut.

*Research supported by Spar Aerospace Limited under Subcontract 30948TC, and by the Natural Sciences and Engineering Research Council of Canada under Grant A-4140.

**Now with Litton Systems Canada Ltd., Toronto.

The EMI estimation procedure involved the following steps:

1) Visual observations to establish the locations and lengths of the arcs, 2) Calculation of the arc current time-derivative from the measured loop antenna signal, 3) Use of the radiation-field formula for a transient current element in order to estimate the radiated field strength when the strut is not close to a large metal surface, 4) Calculation of the broadband radiated emission spectrum at distances appropriate for spacecraft communications antenna pickup, and 5) Comparison with radiated-emission EMI specifications.

Experimental Observations

Discharges were observed at both 3 and 10 nA/cm² current densities. A common type of arc was a bright, straight, thin line about 1 cm long which was the basis for the choice of 1 cm as the current element length for emission calculations. Another common type was a "diffuse discharge" consisting of a sudden jump in specimen luminescence (indicative of charge release) accompanied by antenna signal pickup comparable to the thin-line arc mentioned above. It is possible that the diffuse type of discharge was actually a bright-line type which occurred out of sight on the sides or underside of the strut, but this conjecture was not verified by direct observation. The diffuse and bright-line types of discharge produced similar loop output voltage waveforms. Typically, the strongest recorded antenna signals consisted of positive, roughly triangular pulses followed by appreciably smaller negative overshoots. For purposes of analysis, this shape was approximated as triangular (with a rise time of 3 ns and a fall time of 11 ns), and the negative overshoot was ignored. Two strut specimens were tested, one discharging much less frequently and generating loop voltages about 40% weaker than the other. Two arcs longer than 1 cm were observed, which will be discussed later in this paper.

Estimation of Radiated Field Strength

The azimuthal magnetic field strength H close to a long current I is given at distance ρ by

$$H(t) = \frac{I(t)}{2\pi\rho} \tag{1}$$

The loop voltage v(t) around a highly conducting, small wire loop antenna in a magnetic field with average strength H(t) is given by

$$v(t) = \frac{\partial}{\partial t}\mu_o A\, H(t) \tag{2}$$

$$= \frac{\mu_o A}{2\pi\rho} I'(t) \tag{3}$$

where A is the area of the loop and μ_o the permeability of free space.

Consider a short current element of length ℓ oriented in the Z direction. Then the radiated azimuthal magnetic field strength, H_ϕ, at a distance r perpendicular to the current element is[1]

$$H_\phi(t) = \frac{\ell}{4\pi c r} I'(t) \tag{4}$$

$$= \frac{\ell}{2cr}\cdot\frac{\rho}{\mu_o A} v(t) \tag{5}$$

$$= \frac{\ell\rho}{2\eta r A} v(t) \tag{6}$$

where $c = \frac{1}{\sqrt{\mu_o \varepsilon_o}}$ is the free space velocity of light

and $\eta = \sqrt{\frac{\mu_o}{\varepsilon_o}}$ is the intrinsic impedance of free space.

The uniform plane wave relation $E_\theta = \eta H_\phi$ gives finally

$$E_\theta(t) = \frac{\ell\rho}{2rA} v(t) \quad (7)$$

This formula shows that the radiated E-field pulse has the same shape as the voltage pulse measured by the near-field loop antenna.

The parameters used in the calculations are as follows:

ρ = 8 mm

A = 152 mm²

ℓ = 1 cm

r = 2 m

The value r = 2 m is deduced from spacecraft drawings showing the relative locations of the antennas and the solar array masts. The length ℓ = 1 cm arises from the observation that the visible arcs on the strut were mostly less than 1 cm in length. An inconsistency will be noted in that a long current was assumed in (1) while a relatively short current was assumed in the radiation calculations in (4): for the particular dimensions involved, the use of a short current and the Biot-Savart law to replace (1) produced essentially the same numerical result. The strongest measured pulses had a maximum loop voltage v(t) of 1.3 volts, which results in a predicted maximum $E_\theta(t)$ from (7) of 0.17 V/m. The discharge arc current also may be estimated by assigning the observed typical rise time of 3 ns to the time interval in the derivative in equation (3): consequently, with $\mu_o = 4\pi \times 10^{-7}$ H/m, equation (3) gives the peak value of I(t) to be 1.0 A.

Spectrum Calculations

The spectrum calculation procedure used is the one described in the book by White[2] for trapezoidal and triangular pulses. The typical pulse shape as taken from photographs for analysis is approximately triangular with a rise time τ_r = 3 ns and a fall time τ_f = 11 ns. The time between mid-rise and mid-fall is τ = 7 ns. There is a single negative overshoot consisting of a relatively slower and more rounded triangular pulse with an area less than 1/3 of the positive pulse: this overshoot is ignored in the spectrum calculation but will be commented on later. The E-field spectrum given in the above reference is

$$E(f) = 2\tau\Delta e \frac{\left[e^{j\pi f\tau} \frac{\sin \pi f\tau_r}{\pi f\tau_r} - e^{-j\pi f\tau} \frac{\sin \pi f\tau_f}{\pi f\tau_f} \right]}{2j\pi f\tau} \quad (8)$$

in which Δe is the maximum electric field of 0.17 V/m in the triangular pulse and f is the frequency in Hz. The magnitude of the spectrum can be expressed in the following form which is convenient for calculation:

$$|E(f)| = \frac{\tau\Delta e}{\pi f\tau} \left[A_r^2 + A_f^2 - 2 A_r A_f \cos 2\pi f\tau \right]^{\frac{1}{2}} \quad (9)$$

$$\text{where } A_r = \frac{\sin \pi f\tau_r}{\pi f\tau_r} \text{ and } A_f = \frac{\sin \pi f\tau_f}{\pi f\tau_f}$$

The spectrum S(f) is converted to dB, the magnitude reference is changed from 1 V/m to 1 µV/m, and the bandwidth reference from 1 Hz to 1 MHz by the formula

$$S(f) = 20 \log_{10}|E(f)| + 240 \quad (10)$$

for which the units are dB µV/m/MHz.

The numerical spectrum computation was done using the following values, with the frequency F in MHz replacing f in Hz:

$$\begin{aligned} \pi f\tau_r &= 0.00942\ F \quad \text{for} \quad \tau_r = 3 \text{ ns} \\ \pi f\tau_f &= 0.0346\ F \quad \text{for} \quad \tau_r = 11 \text{ ns} \\ 2\pi f\tau &= 0.0440\ F \quad \text{for} \quad \tau = 7 \text{ ns} \\ \Delta e &= 0.17 \text{ V/m} \end{aligned} \quad (11)$$

The results are shown in Fig.2, along with the specified upper bound on broadband radiated E-field emission. This upper bound is the specification for the Olympus satellite, which is comparable to the RE02 specifications[2].

Discussion of Spectrum

The calculated pulse spectrum just touches the specified upper limit in the 420-450 MHz band, and in the vicinity of 40 MHz the pulse spectrum is 4 dB under the specification. If the negative overshoot were included in the spectrum calculation, the level around 40 MHz would probably be raised slightly (based on the fact that the waveform is such as to contain stronger components near 40 MHz), while the spectrum above 200 MHz would be essentially unaffected. Thus it is clear that the calculated interference spectrum comes very close to the limit in two frequency ranges.

Two arcs were observed to be longer than 1 cm, one noted as approximately 1-2 cm long, and the other noted as 2 cm long. Therefore it could be argued that the length ℓ could be 2 cm rather than the 1 cm used in the calculation, with a consequent 6 dB rise in the spectrum in Fig.2. However the pulse photos for the two longer arcs show longer rise times of 10 ns and 8 ns (compared with 3 ns), longer pulse durations of 20 ns and 16 ns (compared with 14 ns) and pulse shapes which are more rounded. Therefore the spectra would exhibit high-frequency fall-off which is displaced in the direction of lower frequencies, thus reducing the EMC hazard. Thus the graph of Fig.2 might need to be raised a few dB (certainly no more than 6 dB) to cover the worst cases, but it would also have to be shifted somewhat lower in frequency. The net result would be an interference spectrum which either just touches the specified upper limit line or very slightly exceeds it.

In addition to the current flowing on the strut, it is likely that there would be appreciable current ejection into the surrounding space, away from the strut. If such currents were unidirectional, they would have a large dipole moment and would radiate significantly. It is postulated that this is not the case, under the assumption that the electrons are ejected over a wide range of directions and thus have negligible net dipole moment. As an alternative assumption leading to the same conclusion, one could consider the possibility that the ejected electrons return in loops to nearby parts of the spacecraft. These current loops might contribute little to the radiated field because of the fact that a small loop of current radiates appreciably less than a unidirectional current of the same magnitude. Return current conduction through the spacecraft structure is not considered as a possible source of interference, for the purposes of this study which is limited to radiated emission.

Conclusions

The estimated pulse spectrum is very close to the specified upper limit for radiated emission. Because of the choice of a monoenergetic beam and current densities at least an order of magnitude higher than in synchronous orbit, it is estimated that, if an arc occurred in space, it would not likely be stronger than the ones measured, so the fiberglass struts can be regarded as safe with respect to the arc discharge threat, to the degree that the experimental and theoretical procedures used are relevant. However, the proximity of the emission spectrum to the specified upper limit indicates that continued alertness to the arc discharge threat is required.

References

[1] W.E. Waters, Electrical Induction from Distant Current Surges, Prentice-Hall Inc., Englewood Cliffs, N.J., 1983.

[2] D.R.J. White, Electromagnetic Interference and Compatibility, Vol.2 of EMI Test Methods and Procedures, Don White Consultants Inc., Gainesville, Va., 1974.

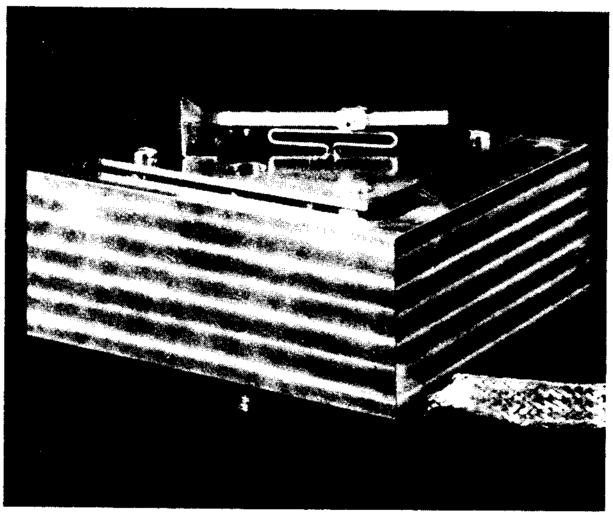

Figure 1a

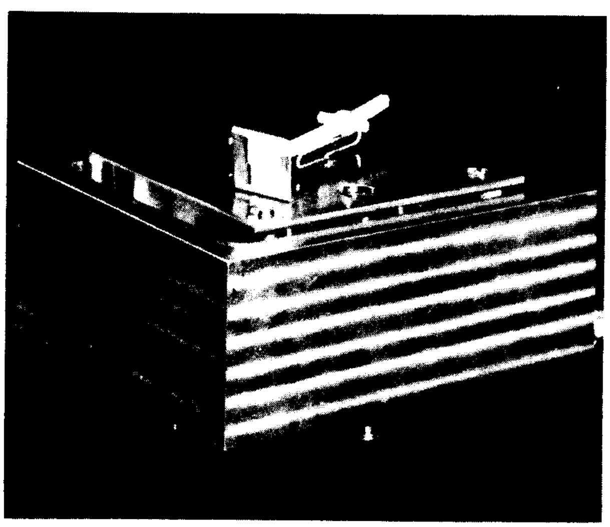

Figure 1b

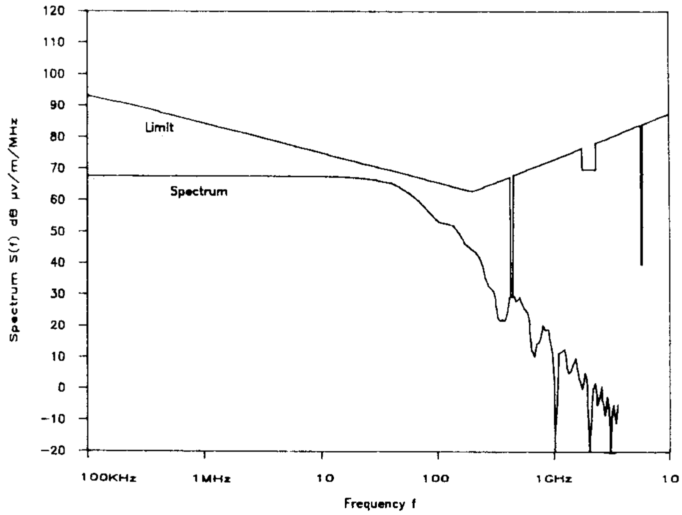

Fig.2 Spectrum of a triangular pulse with a maximum amplitude of 0.17 V/m, a rise time of 3 ns, and a fall time of 11 ns. The broadband radiated E-field emission limit is also shown.